

Thermally self-sufficient process for single-step coproduction of methanol and dimethyl ether by CO₂ hydrogenation

Vaquerizo, Luis; Kiss, Anton A.

DOI

[10.1016/j.jclepro.2024.140949](https://doi.org/10.1016/j.jclepro.2024.140949)

Publication date

2024

Document Version

Final published version

Published in

Journal of Cleaner Production

Citation (APA)

Vaquerizo, L., & Kiss, A. A. (2024). Thermally self-sufficient process for single-step coproduction of methanol and dimethyl ether by CO₂ hydrogenation. *Journal of Cleaner Production*, 441, Article 140949. <https://doi.org/10.1016/j.jclepro.2024.140949>

Important note

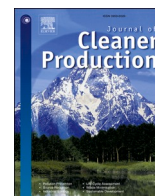
To cite this publication, please use the final published version (if applicable).
Please check the document version above.

Copyright

Other than for strictly personal use, it is not permitted to download, forward or distribute the text or part of it, without the consent of the author(s) and/or copyright holder(s), unless the work is under an open content license such as Creative Commons.

Takedown policy

Please contact us and provide details if you believe this document breaches copyrights.
We will remove access to the work immediately and investigate your claim.



Thermally self-sufficient process for single-step coproduction of methanol and dimethyl ether by CO₂ hydrogenation

Luis Vaquerizo^{a,b}, Anton A. Kiss^{b,*}

^a Institute of Bioeconomy, PressTech Group, Department of Chemical Engineering and Environmental Technology, University of Valladolid, Doctor Mergelina s/n, 47011, Valladolid, Spain

^b Department of Chemical Engineering, Delft University of Technology, Van der Maasweg 9, 2629 HZ, Delft, the Netherlands

ARTICLE INFO

Handling Editor: Panos Seferlis

Keywords:

Process integration
Process design
Dividing-wall column
Energy efficiency
Dual catalyst

ABSTRACT

Methanol and DME are highly efficient fuels and relevant building blocks that can be synthesized by CO₂ hydrogenation. While several alternatives for methanol production by CO₂ hydrogenation have already been developed at a commercial scale, DME production is still based on methanol dehydration. In this sense, the development of bifunctional methanol synthesis/dehydration catalysts is a clear opportunity for the simultaneous coproduction of methanol and DME in a single-step process. Although a few alternatives for DME-methanol coproduction have been proposed, either they need external fuels or refrigerants, or part of the CO₂ used as raw material is purged, resulting in a loss of methanol and DME yields. This work presents a novel thermally self-sufficient process that hydrogenates CO₂ into methanol and DME in a single reactor at 100 % yield (only water as a byproduct at 0.94 kg_{water}/kg_{product}), that only consumes air, cooling water (0.006 m³_{water}/kg_{products}) and electricity (net CO₂ emissions of −1.20 or 0.64 kg_{CO2eq}/kg_{products} when the plant is operated with green or grey electricity, respectively). The innovative design, based on the combination of a top-divided wall column, an integrated heat network, and limited pressure drop in the reaction-separation loop, results in a thermally self-sufficient process that uses only 0.76 kWh per kg products.

1. Introduction

The introduction of this research work is divided into five paragraphs that present the current state of the art on DME production and the main challenges of developing an alternative for DME production by CO₂ hydrogenation. The first paragraph outlines the advantages of methanol and DME as clean substitutes for conventional fuels. The second paragraph presents the basics of the conventional DME production process and some existing intensified alternatives, highlighting the reasons that prove the importance of developing a single-step DME production process by CO₂ hydrogenation. The third and fourth paragraphs introduce the currently published works on DME production by CO₂ hydrogenation, showing the main challenges of the process. Finally, the last paragraph presents the main innovations of the process developed in this research work focusing on how the main challenges of DME production by CO₂ hydrogenation are addressed.

Methanol and derived dimethyl ether (DME) are excellent transportation fuels and convenient starting materials for the production of light olefins. Both compounds can be synthesized by hydrogenation of

captured CO₂ converting carbon dioxide, a greenhouse gas, into a renewable carbon source [Olah et al. \(2009\)](#). From all the available CO₂ capture technologies, this work considers that CO₂ is recovered by amine absorption, as this technique is the most mature technology when compared with other existing techniques such as CO₂ adsorption, membrane separation, and cryogenic distillation ([Leung et al., 2014](#)). Although this work is focused on CO₂ utilization, it is also worth noting that the geological storage of CO₂ is also fundamental for the reduction of CO₂ emissions into the atmosphere. In this sense, CO₂ storage by hydrate formation is one of the most feasible alternatives ([Hassanpouryouzband et al., 2020](#)). The hydrogenation of CO₂ into methanol and DME, apart from contributing to the abatement of CO₂ emissions, provides an efficient solution for energy storage. One of the main challenges for the development of a successful hydrogen economy is hydrogen storage. The conversion of hydrogen, a very low-density gas (0.084 kg/m³), into more dense fuels, together with other alternatives such as its geological storage, provides flexibility, in terms of energy availability, when the renewable energy production capacity has dropped (low-sun, low-wind situations) ([Hassanpouryouzband et al., 2021](#) &

* Corresponding author.

E-mail addresses: TonyKiss@gmail.com, A.A.Kiss@tudelft.nl (A.A. Kiss).

<https://doi.org/10.1016/j.jclepro.2024.140949>

Received 18 November 2023; Received in revised form 20 January 2024; Accepted 25 January 2024

Available online 31 January 2024

0959-6526/© 2024 The Authors. Published by Elsevier Ltd. This is an open access article under the CC BY license (<http://creativecommons.org/licenses/by/4.0/>).

2022). While methanol can efficiently store the energy used to produce hydrogen by water electrolysis [Lee et al. \(2020\)](#), DME has been identified as an ultraclean alternative for diesel engines, as its combustion does not produce NO_x, smoke, or particulates ([Fleisch et al., 1997](#); [Lotfollahzade Moghaddam and Hazlett, 2023](#)).

DME has been conventionally produced in a two-step chemical process that involves first the conversion of syngas into methanol and then the dehydration of methanol into DME. This process, apart from requiring two catalytic reactors ([Peinado et al., 2024](#)), suffers from equilibrium limitations in the methanol synthesis reactor ([Zhang et al., 2015](#)). In this sense, extensive work has been done to improve or intensify the conventional DME production process. [Luyben \(2017\)](#) improved the original DME production process presented by [Turton et al. \(2003\)](#) by including an economizer, a vaporizer, and a steam generator, saving 38 % in energy costs. [Bildea et al. \(2017\)](#), [Kiss and Suszwalak \(2012\)](#), and [Gor et al. \(2020\)](#), intensified the DME production process in a single reactive distillation column and in reactive dividing wall columns, leading to savings of up to 30 % in CapEx and up to 60 % in energy requirements. Although these works have reduced the production cost of DME, they still rely on the use of methanol as raw material. Thus, there is still a lack of research on the DME production directly from CO₂. The single-step conversion of a mixture of CO₂ and H₂ into DME is very attractive, as it only needs a single catalytic reactor for the whole process, and the equilibrium limitations related to methanol production are overcome. In this sense, the use of bifunctional (dual) catalysts that combine a methanol synthesis catalyst and a methanol dehydration catalyst has been recently explored by some authors ([Diban et al., 2014](#); [Vu et al., 2021](#)), and [Wild et al. \(2022\)](#), concluding that although there is enormous potential to increase the activity and selectivity of these catalysts, using commercial methanol synthesis and dehydration catalysts it is already possible to reach CO₂ conversions of up to 47 %. The key benefit of bifunctional catalysts is the fact that both the methanol synthesis reaction and the methanol dehydration reaction to DME can be carried out in a single reactor. This allows for increasing the equilibrium conversion of the first reaction, as the methanol produced in the synthesis reaction is consumed in the dehydration reaction. This is one of the main limitations of the conventional route for DME production relying on methanol as raw material. The use of bifunctional catalysts allows for increasing the overall efficiency of the plant. In single-step reactors loaded with bifunctional catalysts, the equilibrium conversion is reached faster resulting in a smaller reactor and a reduction in the amount of catalyst required to obtain the same productivity as in a two-step process. Apart from the increase in the equilibrium conversion ([Banivaheb et al., 2022](#)), the use of a single-step reactor increases the thermal efficiency of the plant, as the two preheating trains required for methanol and DME synthesis (when the synthesis is performed in a two-step process) are combined in a single preheating train. Moreover, in the conventional two-step process, the outlet of the methanol synthesis reactor is cooled down before the separation section, and then the produced methanol is heated up again before the dehydration reactor, resulting in thermal inefficiency. The motivation behind developing a single-step coproduction process for methanol and DME by CO₂ hydrogenation is the possibility of obtaining a thermally self-sufficient process in which the CO₂ emissions are limited to those related to the capture of the CO₂ and the production of the H₂ consumed in the reactor, and to the production of the power required in the plant, that converts CO₂, a greenhouse gas into renewable fuels.

Although the conversion of captured CO₂ into methanol or DME using electrolytic hydrogen is gaining attention among the scientific community, there is still a small number of publications addressing this process. [Poto et al. \(2023\)](#), presented a techno-economic assessment of a one-step conversion process using a membrane-assisted reactor. The use of membrane reactors allowed for removing the water produced in the methanol and DME synthesis reactions, shifting the equilibrium towards the formation of DME. Although the CO₂ single pass conversion in the reactor increased up to 55 %, the process consumes natural gas and a

refrigerant penalizing its environmental sustainability. [Michailos et al. \(2019\)](#) developed a two-step DME production process by CO₂ hydrogenation. Although the authors were able to convert 83.2 % of the CO₂ into DME, the process is not thermally self-sufficient and consumes natural gas. Finally, [Dikić et al. \(2023\)](#) proposed a separation process based on the recovery of CO₂ in a high-pressure hydrogen stripper. Although this is an efficient way of separating CO₂ from the heavier products (DME, MeOH, and water), two additional distillation columns are required for DME-MeOH-water separation.

Although some process alternatives on CO₂ hydrogenation to methanol and DME have been already proposed, either they depend on external fuels or refrigerants, they include purge streams that reduce the overall yield of the process, or they are based on two-step processes that need two catalytic reactors and are affected by equilibrium limitations in the methanol synthesis reactor. Finding a single-step, thermally self-sufficient process for methanol and DME coproduction that does not require the use of refrigerants for DME condensation, minimizing the power consumption, and maximizing the overall yield is fundamental for the development of an environmentally sustainable methanol-DME coproduction process with a competitive production cost.

This work is based on the results of a simulation that includes experimentally validated kinetics and equilibrium correlations which were reported in detail by [Kiss et al. \(2016\)](#), [Wild et al. \(2022\)](#), [Graaf et al. \(1986\)](#), and [Aguayo et al. \(2007\)](#). It presents a novel thermally self-sufficient process for the clean, integrated coproduction of methanol and DME in a single reactor, that does not require the consumption of any external fuel or refrigerant (only cooling water and air), that maximizes the product yields by recovering all the unreacted CO₂ in a top dividing-wall column (DWC), that reduces the power consumption by restricting the pressure loss in the reaction-separation-recycle loop to the pressure drop in the circuit, and that obtains high-purity methanol and DME in a two-step intensified separation process based on the combination of the top DWC used for CO₂ recovery and an additional distillation column. The key outcome of this work is the development of a sustainable process that converts CO₂ into methanol and DME without CO₂ emissions related to the production of heating sources, as the process is thermally self-sufficient (using only green electricity), uses cooling water as cooling fluid, with minimum power consumption in the compressors of the plant, and proposing for the first time a combination of a top dividing wall column and a distillation column to recover the unreacted CO₂ while obtaining at the same time high purity DME, methanol, and water streams. The feed stream flowrates are the same as those used in our previous CO₂ to methanol processes ([Kiss et al., 2016](#); [Vaquerizo and Kiss, 2023](#)) (100 ktpy methanol plants) to allow a direct comparison with the results of these works.

2. Problem statement

A sustainable, single-step coproduction of DME and methanol by CO₂ hydrogenation depends on finding a clean alternative that does not rely on the consumption of external fuels or refrigerants (as this would result in additional CO₂ emissions), that minimizes the power consumption in the plant (to reduce the CO₂ emissions related to power production), and that maximizes the methanol and DME yields (to avoid CO₂ purges). Although a few alternatives have been recently proposed, either they depend on the consumption of external fuels and refrigerants or they include purge streams ([Poto et al., 2023](#); [Michailos et al., 2019](#)). On the other hand, the process presented in this research work is thermally self-sufficient, thanks to its thermally integrated heat exchanger network that utilizes the enthalpy of the reaction products and the heat of reaction to cover all the heat necessities of the process, reaches maximum yield, as there is no purge whatsoever and the reagents are completely converted in reaction products, and uses a combination of a top dividing wall column that acts both as a stripper, recovering on its prefractionator side the unreacted CO₂, and as a fractionator, obtaining at the top of its fractionator side a high-purity DME stream and at the

bottoms of the column a mixture of methanol and water with traces of CO₂ and DME, which is separated in a second distillation column to obtain high-purity methanol and water streams. The top dividing wall column is a 22-stage column that operates at 23 bar, as this is slightly higher than the discharge pressure at the third stage of the CO₂ compressor where the CO₂-rich stream is recycled, which uses cooling water to condense the overhead vapors of the prefractionator side, setting a saturation temperature of 40 °C to reduce the amount of DME in the recycling stream. The operating pressure corresponds also with a saturation temperature of 67 °C for the DME recovered on the fractionator side, allowing for the use of either cooling water or air as cooling fluids in the fractionator side condenser. Finally, the reboiler of the column is thermally integrated with the hydrogenation reactor, using the high-pressure steam generated in the reactor as a heating fluid. On the other hand, the methanol-water distillation column is a 33-stage column that obtains high-purity methanol and water, operates practically at the atmospheric pressure, can use either cooling water or air as cooling fluids in the condenser (as the condensation temperature is equal to 67 °C), and is thermally integrated with the reaction products, which provide the duty required in the column reboiler. Compared with previously proposed works (Poto et al., 2023; Michailos et al., 2019) this process does not require the consumption of natural gas nor the use of a refrigerant, as the process is thermally self-sufficient and only uses cooling water and air as cooling fluids. In terms of efficiency, this process results in a higher production yield – 99.97 % mol vs 99.62 % mol in the case of Poto et al. (2023) and 94.59 % mol in the case of Michailos et al. (2019) – and has higher energetic efficiency, as it presents a lower electrical power consumption – 0.49 kWh_e/kg_{products} vs 0.71 kWh_e/kg_{products} in the case of Poto et al. (2023) and 0.90 kWh_e/kg_{products} in the case of Michailos et al. (2019) – and does not require the use of any external fuel or refrigerant. Moreover, while the previous processes proposed by Poto et al. (2023) and Michailos et al. (2019) require three distillation columns, and in the case of Michailos et al. (2019), two hydrogenation reactors, in this work, both methanol and DME are synthesized, and purified in a single hydrogenation reactor and two distillation columns, resulting in a lower CAPEX investment. The higher methanol and DME yields of this process, the better energetic efficiency, and the lower CAPEX of the plant are expected to result in a lower production cost for methanol and DME.

3. Process simulation basis

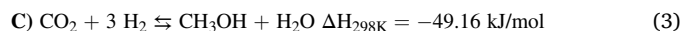
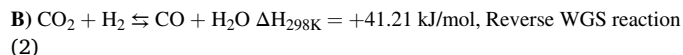
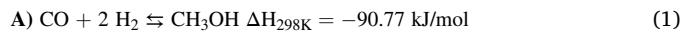
This section presents the simulation basis for a DME and methanol production plant by CO₂ hydrogenation. A fibrous Cu/Zn/Al/Zr catalyst (An et al., 2009), which is very similar to the commercial methanol synthesis catalysts, and the commercial ferrierite-type zeolite H-FER 20 (Wild et al., 2022) used for methanol dehydration to DME are considered in this work.

3.1. Property model

The process was rigorously simulated in Aspen Plus using the Predictive Soave-Redlich-Kwong (PSRK) property method which predicts the binary interactions by combining UNIFAC with the Huron-Vidal mixing rules and the Soave-Redlich-Kwong equation of state. This method, suitable for polar compounds (DME, methanol, and water) and high operating pressures and temperatures (pressure up to 65 bar and temperature up to 250 °C) provides the most accurate representation of the CO₂ solubility in DME, methanol, and water (Dikić et al., 2023). All the required binary interaction parameters are available in the Aspen Plus databanks (e.g. APV-120 EOS-LIT). As there is a small liquid split in the DME-methanol-water ternary diagram, the distillation columns where these three components are present must be modeled allowing for the existence of a secondary liquid phase (VLE model).

3.2. Chemical reactions

The chemistry of methanol production by CO₂ hydrogenation involves three main equilibrium reactions (A, B, and C) where water is also produced as a by-product (Fiedler et al., 2005):



On the other hand, DME is produced by methanol dehydration following the next equilibrium-limited reaction (D) that also involves water as a byproduct (Müller and Hübsch, 2000; Lei et al., 2011):



In the case of methanol production, higher methanol yields are obtained by operating at lower reaction temperatures and higher reaction pressures (Dimian et al., 2019; Kanuri et al., 2022). Moreover, as explained in our previous works (Vaquerizo and Kiss, 2023; Kiss et al., 2016), the optimum stoichiometric number (SN) is equal to 2, meaning a molar (H₂/CO₂) feed ratio of 3:1 when only CO₂ and H₂ are present. The SN number is calculated as follows:

$$\text{SN} = \frac{y_{\text{H}_2} - y_{\text{CO}_2}}{y_{\text{CO}} + y_{\text{CO}_2}} \quad (5)$$

In the case of DME, the equilibrium conversion increases when operating the reactor at lower temperatures. In this case, the reaction is not affected by the pressure, as there is no change in the number of moles in the methanol dehydration reaction. Finally, higher methanol concentrations increase DME production as the methanol dehydration reaction produces DME while consuming methanol (Azizi et al., 2014).

The overall process is thermodynamically favored by high pressures (higher methanol production, no effect on DME production), low temperatures (higher DME and methanol equilibrium conversions), and a molar (H₂/CO₂) feed ratio of 3:1 (higher methanol production and therefore, higher DME production).

3.3. Chemical equilibrium

The correlations used in this work to calculate the equilibrium constants (K_A , K_B , and K_C) were provided by Kiss et al. (2016) and derived from an Aspen Plus equilibrium reaction. These correlations, validated against the expressions reported by Lim et al. (2009) derived from the experimental data from Graaf et al. (1986), are [Pa] base expressions, as they are required in this form to be implemented in the driving force term of the kinetic equations.

$$\begin{aligned} \ln K_A &= \frac{9.8438 \times 10^4}{RT} - 29.07 \rightarrow K_A = 2.3717 \\ &\times 10^{-13} \exp\left(\frac{9.8438 \times 10^4}{RT}\right) [\text{atm}^{-2}] \\ \ln K_A &= -52.096 + \frac{11840}{T}; \text{ with } K_A [\text{Pa}^{-2}] \end{aligned} \quad (6)$$

$$\begin{aligned} \ln K_B &= \frac{-4.3939 \times 10^4}{RT} + 5.639 \rightarrow K_B = 2.8118 \\ &\times 10^2 \exp\left(\frac{-4.3939 \times 10^4}{RT}\right) [-] \\ \ln K_B &= 5.639 + \frac{-5285}{T}; \text{ with } K_B [-] \end{aligned} \quad (7)$$

$$K_C = K_A \times K_B \rightarrow K_C = 6.6688 \times 10^{-11} \exp\left(\frac{5.4499 \times 10^4}{RT}\right) [\text{atm}^{-2}]$$

$$\ln K_C = -46.457 + \frac{6555}{T}; \text{ with } K_C [Pa^{-2}] \quad (8)$$

In the case of DME production, Aguayo et al. (2007) regressed the equilibrium constant for the methanol dehydration reaction to DME from experimental data. Bildea et al. (2017) reported an expression derived from Aspen Plus using a Gibbs reactor that shows excellent agreement with the correlation of Aguayo et al. (2007).

$$\ln K_D = -2.6305 + \frac{2787}{T}; \text{ with } K_D [-] \quad (9)$$

3.4. Catalyst and kinetics

This work uses a bifunctional catalyst that is a combination of a methanol synthesis catalyst (Cu/Zn/Al/Zr) and a dehydration catalyst (H-FER). The use of a bifunctional catalyst allows for converting CO₂ into DME in a single step, avoiding thermodynamic limitations related to the equilibrium conversion of the first reaction and increasing the overall efficiency of the process. The volumetric methanol synthesis/methanol dehydration catalyst ratio was fixed at 95.5 %wt according to the results reported by Wild et al. (2022). This catalyst proportion ensures that both methanol formation and dehydration are running close to equilibrium.

This work considers the methanol production catalyst and kinetic model from Kiss et al. (2016), based on the A3B2C3 kinetic model tested by Graaf et al. (1988) combined with the kinetic data from An et al. (2009). This model was proven as the best kinetic model of the 48 models tested by Graaf et al. (1988). It assumes that CO and CO₂ adsorb competitively on the first active sites (called s1-sites), that H₂ and H₂O are adsorbed competitively on the second active sites (s2-sites), that the adsorption of methanol is negligible, and that H₂ adsorbs dissociatively. This model can distinguish between CO and CO₂ adsorption, as it assumes that both compounds adsorb competitively. This means a better representation of the reactor performance and therefore, a better selection of the operating conditions and amount of catalyst required to reach equilibrium. The experimental data from An et al. (2009) was obtained for a fibrous Cu/Zn/Al/Zr catalyst selected in this work since, unlike other commercial catalysts, this catalyst was specially designed for methanol production by CO₂ hydrogenation. This catalyst is similar to the CuO/ZnO/ZrO₂ catalyst used by Wild et al. (2022), but the derived kinetic model for this catalyst is not based on a lumped approach thus providing a more accurate representation of the methanol synthesis kinetics (Kiss et al., 2016).

All the required input data for the kinetic equations using the Aspen Plus format are provided in Table 1, Table 2, and Table 3. The corresponding rate equations for the kinetic model are:

$$r_{CH_3OH,A3} = k_A \frac{K_{CO} [f_{CO} f_{H_2}^{3/2} - f_{CH_3OH} / (K_A \sqrt{f_{H_2}})]}{(1 + K_{CO} f_{CO} + K_{CO_2} f_{CO_2}) [\sqrt{f_{H_2}} + (K_{H_2O} / \sqrt{K_H}) f_{H_2O}]} \quad (10)$$

$$r_{CO,B2} = r_{H_2O,B2} = k_B \frac{K_{CO_2} [f_{CO_2} f_{H_2} - f_{H_2O} f_{CO} / K_B]}{(1 + K_{CO} f_{CO} + K_{CO_2} f_{CO_2}) [\sqrt{f_{H_2}} + (K_{H_2O} / \sqrt{K_H}) f_{H_2O}]} \quad (11)$$

Table 1

Kinetic factor for reactions A, B and C (based on data from An et al. (2009)) – the units used are [Pa] for fugacity and [mol/g_{catalyst} s] = [kmol/kg_{catalyst} s] for reaction rate.

| Reaction | k | n | Ea [J/mol K] |
|----------|--|---|--------------|
| A | 4.0638×10^{-6} [kmol/kgcat s Pa] | 0 | 11,695 |
| B | 9.0421×10^8 [kmol/kgcat s Pa ^{1/2}] | 0 | 112,860 |
| C | 1.5188×10^{-33} [kmol/kgcat s Pa] | 0 | 266,010 |

Table 2

Constants for driving force (from An et al. (2009)) using the format for Aspen Plus.

| Reaction | K1 | | K2 | |
|----------|--------|--------|--------|--------|
| | A | B | A | B |
| A | -23.20 | 14,225 | 28.895 | 2385 |
| B | -22.48 | 9777 | -28.12 | 15,062 |
| C | -22.48 | 9777 | 23.974 | 3222 |

Table 3

Ki factors for adsorption term (terms 2, 3, 5 from An et al. (2009); rest is explicitly derived by calculation).

| Term | Expression | A _i = ln (a _i) | B _i = b _i /R | [[c] _i ^{b_i} |
|------|--|---------------------------------------|------------------------------------|--|
| 1 | 1 | 0 | 0 | $\sqrt{f_{H_2}}$ |
| 2 | $\frac{K_{H_2O}}{\sqrt{K_H}}$ | -26.1568 | 13,842 | f_{H_2O} |
| 3 | K_{CO} | -23.2006 | 14,225 | $f_{CO} \sqrt{f_{H_2}}$ |
| 4 | $\frac{K_{CO} K_{H_2O}}{\sqrt{K_H}}$ | -49.3574 | 28,067 | $f_{CO} f_{H_2O}$ |
| 5 | K_{CO_2} | -22.4827 | 9777 | $f_{CO_2} \sqrt{f_{H_2}}$ |
| 6 | $\frac{K_{CO_2} K_{H_2O}}{\sqrt{K_H}}$ | -48.6395 | 23,619 | $f_{CO_2} f_{H_2O}$ |

$$r_{CH_3OH,C3} = r_{H_2O,C3} = k_C \frac{K_{CO_2} [f_{CO_2} f_{H_2}^{3/2} - f_{H_2O} f_{CH_3OH} / (f_{H_2}^{3/2} K_C)]}{(1 + K_{CO} f_{CO} + K_{CO_2} f_{CO_2}) [\sqrt{f_{H_2}} + (K_{H_2O} / \sqrt{K_H}) f_{H_2O}]} \quad (12)$$

In the case of DME synthesis, this work uses the kinetic model from Wild et al. (2022). The kinetic model was derived from experimental data obtained for an H-FER commercial catalyst. This catalyst was proven to be an excellent catalyst for methanol dehydration in bifunctional catalyst, as demonstrated by Wild et al. (2022). All the required input data for the kinetic equations using the Aspen Plus format are provided in Table 4. The corresponding rate equation for the model is:

$$r_{DME} = k_D \frac{f_{MeOH}^2 - \frac{1}{K_D} f_{DME} f_{H_2O}}{1 + K_D f_{MeOH}} \quad (13)$$

4. Results and discussion

4.1. Sensitivity analysis

The effect of the reaction pressure (1–100 bar), reaction temperature (200–300 °C), reagents ratio (H₂–CO₂ ratio: 3–9), and catalyst loading (GHSV: 0.1–10⁴ m³/kg_{cat}·h) on the reactor performance is analyzed by plotting the variation of the DME and methanol yields against these

Table 4

Kinetics for the MeOH dehydration reaction (Wild et al., 2022).

| Kinetic Factor | | | | |
|-----------------|--|------------------|-----------------|-------------------|
| | k_D | n | E_a [J/mol·K] | |
| | 0.0218 [kmol/kgcat·s·Pa ²] | 0 | 0 | |
| Driving Force | | | | |
| | A | B | C | |
| K1 | -23.0259 | 0 | 0 | |
| K2 | -12.5069 | -3130.4 | -1.148 | |
| Adsorption Term | | | | |
| Term | Expression | $A_i = \ln(a_i)$ | $B_i = b_i/R$ | $\prod c_j^{b_j}$ |
| 1 | 1 | 0 | 0 | 1 |
| 2 | K_θ | -7.54414 | 0 | f_{MeOH} |

process parameters. These are the typical range of process conditions used in methanol synthesis by CO₂ hydrogenation (Vaquerizo and Kiss, 2023; Kiss et al., 2016). Fig. 2 shows that the DME and methanol yields increase with pressure. This can be easily explained by the fact that methanol production by CO or CO₂ hydrogenation proceeds with a decrease in the number of moles. Moreover, Figs. 2 and 3 show that for a fixed amount of catalyst, the reaction conversion is kinetically limited in the low-temperature operating range and equilibrium limited in the high-temperature operating range. Thus, there is an operating window in which the methanol and DME yields increase with the H₂/CO₂ ratio and the operating pressure. Fig. 4 shows that at 250 °C, the reaction is equilibrium limited when the GHSV is lower than 2 m³/kg_{cat}·h. In this work, an operating temperature of 250 °C and a GHSV of 1.5 m³/kg_{cat}·h have been selected as these operating parameters provide a trade-off between the amount of catalyst required in the reactor and the equilibrium conversion reached. Regarding the operating pressure in the reactor, an increase in this parameter means higher equilibrium conversion and heat generation, lower reactor volume, and higher DME recovery in the flash (FLASH-1). A higher heat generation means that the reagents can be heated up to the reactor inlet temperature (220 °C) providing more duty in the HEATER (as it uses the steam generated in the reactor) while reducing, at the same time, the duty in the FEHE. Lowering the duty in the FEHE means higher LMTD in the HEATER, FEHE, DC-REBOILER, and vaporizer (VAP), and therefore, a lower total heat transfer area. Regarding the reactor volume, higher pressure means higher gas density and therefore, the same space velocity with more mass of reagents per tube or, in other words, fewer tubes required in the reactor.

Finally, increasing the operating pressure in the reactor results in more DME and CO₂ recovery in the FLASH-1. Although a higher DME recovery means lower recycling and therefore a smaller reactor volume, since more CO₂ is recovered in the flash liquid stream, more CO₂ is sent to the DWC and a higher duty is required in the DWC reboiler.

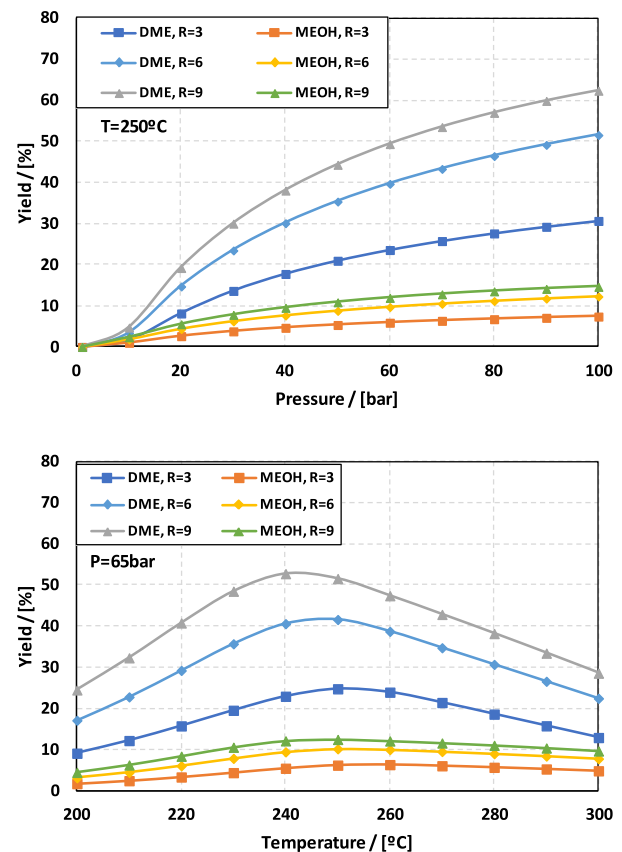


Fig. 2. Effect of pressure on the DME and MeOH yield, at fixed temperature and various reactants ratios (top), and effect of temperature on the DME and MeOH yield, at fixed pressure and various reactants ratios (bottom).

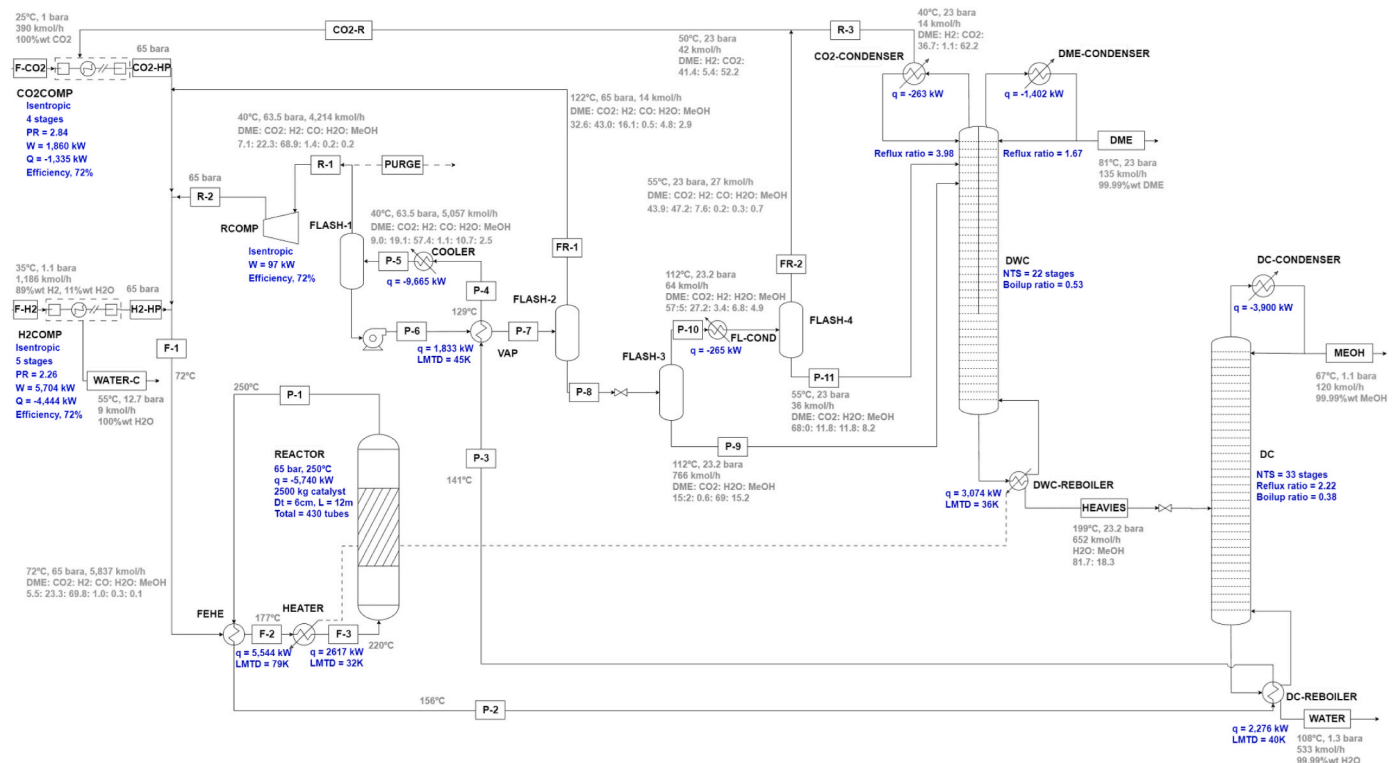


Fig. 1. Process flow diagram of a thermally self-sufficient process for DME and methanol coproduction by CO₂ hydrogenation.

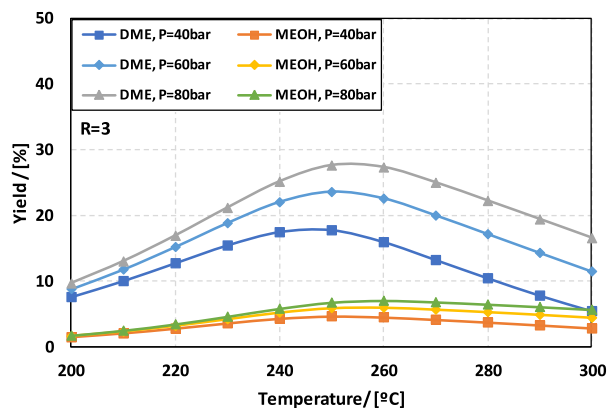


Fig. 3. Effect of temperature on the DME and MeOH yield, at fixed reactants ratio and various pressures.

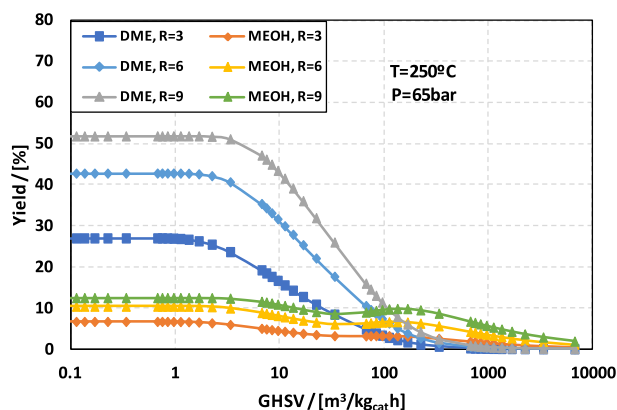


Fig. 4. Effect of the catalyst loading on the DME and MeOH yield, at various reactants ratios and fixed pressure and temperature.

4.2. Process design and simulation

4.2.1. Process description

The DME-methanol coproduction process presented in this work is based on the classical raw materials conditioning, reaction, recycling of unreacted reagents, and product separation scheme (Fig. 1). First, two multistage compressors increase the pressure of the CO₂ and H₂ feed streams from 1.1 bar to 65 bar. This pressure, in combination with the selected reaction temperature (250 °C) provides a compromise between the amount of catalyst required in the reactor and the equilibrium conversion reached. The minimum number of compression stages (4 in the case of the CO₂ compressor, and 5 in the case of the H₂ compressor), has been selected to avoid exceeding a discharge temperature of 176 °C, which is considered the maximum allowable temperature (MAT) for the compressors according to the recommendations of Giampaolo (2010). Exceeding the compressor maximum allowable temperature (MAT) would mean risking the mechanical integrity of the compressor and, at the same time, increasing the compression power, as the compression pathway would diverge more from the isentropic pathway. An interstage temperature of 55 °C has been selected considering air as cooling fluid, that the plant is located in a place where the maximum ambient temperature is 45 °C, and that a minimum temperature difference of 10 °C between air and the process fluid must be maintained in the heat exchangers. Reducing the interstage temperature to 55 °C allows for not exceeding the MAT in the next compressor stage and, at the same time, increases the compression efficiency, since the compression pathway is

closer to the isentropic pathway. If cooling water is used instead of air, the interstage temperature could be reduced even further, decreasing the power consumption in the compressors but increasing the cooling water consumption in the plant. In the case of the H₂ compressor, since a wet hydrogen stream is used as a feed stream, part of the water contained in this stream condenses and is recovered in the interstage KO drums. On the other hand, there is no interstage condensation in the CO₂ compressor. This compressor receives an interstage feed stream in its fourth stage which results from the combination of the overhead vapor from the fourth flash (FLASH-4) and the uncondensed vapors in the DWC prefractionator condenser (CO₂-CONDENSER). As both the hydrogen and the CO₂ compressors are driven by green electricity, if it is not possible to ensure a constant supply of green electricity to the plant, an additional and more stable backup power source would be also needed.

The compressed CO₂ stream is mixed with the recycling stream coming from the second flash (FLASH-2), with the recycling stream coming from the recycling compressor (RCOMP), and with the hydrogen stream coming from the hydrogen makeup compressor (H2COMP). The resulting stream is sent to the hydrogenation reactor (REACTOR), which is first heated in a feed-effluent heat exchanger (FEHE) and then in a steam heater (HEATER). While the FEHE recovers heat from the effluent stream (heating the reagents and cooling, at the same time, the products), the HEATER adjusts the inlet temperature of the reagents to 220 °C, maintaining a minimum LMTD of 15 °C with the saturation temperature of the steam produced in the hydrogenation reactor (235 °C), which is used as heating fluid in this exchanger. For the startup of the plant, an external heat supply source is needed to reach a reactor feed stream temperature close to the normal operating temperature (220 °C). Once this temperature is reached, the process becomes thermally self-sufficient. During startup, steam is fed to the HEATER increasing the temperature of the reagents. At the very beginning, the reaction kinetics is very slow, and almost no reaction products nor heat are generated. Once the inlet temperature of the reagents reaches a temperature around 180 °C, the reaction can proceed without the necessity of using external steam (since the reaction is exothermic), and the process achieves its thermally self-sufficient nature.

The hydrogenation reactor is a catalytic multitubular plug-flow reactor operated isothermally at 250 °C using high-pressure boiler feed water as cooling fluid. This temperature provides a compromise between the equilibrium conversion and the amount of catalyst needed. The heat released in the reactor is absorbed by the high-pressure boiler feed water generating the high-pressure steam used as heating fluid both in the HEATER and the DWC reboiler. The 430 tubes of the reactor (D = 6 cm, L = 12m) are charged with 2500 kg of a mixture of Cu/Zn/Al/Zr catalyst as methanol production catalyst and H-FER catalyst for methanol dehydration to DME (bed voidage = 0.98). This amount of dual catalyst ensures that the equilibrium conversion is reached in the reactor. From an operational point of view, the reaction temperature is adjusted by tuning the flow of boiler feed water fed to the hydrogenation reactor. On the other hand, the reaction pressure is adjusted by throttling a control valve located at the outlet of the reactor. The catalyst composition and load are adjusted and charged in the reactor at the beginning of the operation (before the startup of the plant) to achieve maximum DME yield. The reaction pressure (65 bar) temperature (250 °C) and catalyst load (2500 kg) were selected based on the results of the sensitivity analysis presented in this work (Figs. 2–4, and the results of our previous works (Vaquerizo and Kiss, 2023). These values provide a compromise between the equilibrium conversion achieved in the process and the catalyst load. Finally, the catalyst composition was selected based on the studies of Wild et al. (2022), who reported that with a 95 %wt methanol synthesis catalyst and 5 %wt methanol dehydration catalyst ratio, both reactions run at equilibrium.

The reaction products are used as the heat source in the FEHE, with a cold side outlet temperature of 156 °C to increase the LMTD in this gas-gas exchanger (79K), the distillation column reboiler (DC-REBOILER, 36K), and the vaporizer (VAP, 15K). Any increase in the operating

pressure of the reactor will result in a higher equilibrium conversion and therefore a higher heat release. This extra amount of heat can be used in the HEATER, increasing the LMTD in the FEHE, the DC-REBOILER, and the vaporizer (VAP), reducing their corresponding areas. Finally, a trim cooler (COOLER) cools down the reactor effluent to 40 °C using cooling water, to maximize the amount of DME and methanol recovered and sent to the separation section. In this work, it is considered that cooling water must return at 35 °C to the cooling tower and that a minimum temperature difference of 5 °C between the process fluid and the cooling water must be maintained. In the same way, it is considered that the minimum cooling that can be reached using air is 55 °C. If the plant is located in an arid region where no cooling water is available, the last trim cooler could be replaced by an air cooler exchanger, resulting in a higher outlet temperature. Thus, a lower amount of DME and methanol will be recovered and sent to the separation section, increasing the recycling compressor power and decreasing the equilibrium conversion in the hydrogenation reactor.

After the COOLER, the vapor and liquid phases of the reactor effluent stream are separated in a flash (FLASH-1). The overhead vapor stream is recompressed in the recycling compressor (RCOMP) and mixed with the CO₂ and H₂ makeup streams. If the purity of the feed streams decreases and inert or undesirable compounds are present in the feed streams, a small purge is required (typically less than 1 %, but dependent on the amount of impurities). In this case, the overall yield would decrease, as part of the reagents and reaction products would be purged from the process, the compression power would increase, as larger volumetric flowrates are compressed to get the same methanol and DME productions, and, depending on the concentration of impurities, the size of some pipes and pieces of equipment may also slightly increase. Although the CO₂ consumed in the process will come from either a bioprocess or a pretreatment process that ensures that there are no impurities that can damage the catalyst, if any other impurity is present in the feed streams, the control system of the plant will respond accordingly to mitigate its impact in the process performance. The expected impurities, mainly methane or other volatile compounds, will accumulate in the reaction loop, increasing progressively the reaction pressure. A pressure controller will then start to open a pressure control valve located in the purge line, relieving the overpressure by purging the accumulated impurities. If sulfur or other reacting compounds may be present in the feedstock, both analyzers and guard beds will be installed before the CO₂ compressor to ensure that the impurities do not reach the reactor, poisoning the catalyst. Since there is no expansion valve in the reaction loop, the recycling compressor only needs to account for the pressure drop in the circuit. On the other hand, the liquid product stream is compressed first in a pump which is intended to account also for the pressure drop in the reaction loop. After the pump, this stream is heated up (122 °C) and partially vaporized ($x_{\text{vap}} = 0.02$ mol/mol) in the vaporizer (VAP), cooling, at the same time, the reactor effluent stream to 129 °C. The resulting vapor stream, separated in the second flash (FLASH-2), is recycled and mixed with the CO₂ feed stream. On the other hand, the resulting liquid stream is expanded to 23 bar. This pressure, which is slightly higher than the third-stage discharge pressure of the CO₂ compressor, allows for recycling the overhead vapor stream of the fourth flash (FLASH-4) and the non-condensed gases of the DWC prefractionator condenser (CO2-CONDENSER) directly to the fourth stage of the CO₂ compressor. The vapor and liquid streams generated in the expansion are separated in a third flash (FLASH-3). While the vapor phase is cooled down to 55 °C in a flash condenser (FL-COND) using air to recover part of the DME and methanol contained in the stream, the liquid stream is fed to the DWC (tray 6). The two-phase stream obtained after the flash condenser is sent to the last flash (FLASH-4). While the resulting vapor stream is recycled and mixed with the CO2-CONDENSER vapor stream, the resulting liquid stream is fed to the DWC (tray 5).

The top dividing wall column (DWC) located after the recycling section has a double function: recovering in the prefractionator section the unreacted CO₂ (sending it back to the fourth stage of the CO₂

compressor), and obtaining in the main section a purified DME stream (>99.99 % mass). The column, operated at 23 bar (slightly higher than the discharge pressure at the third stage of the CO₂ compressor), has two separated condensers. While the prefractionator partial condenser uses cooling water as cooling fluid to minimize the amount of DME recycled to the CO₂ compressor, the DME-CONDENSER is operated with air, as the saturation temperature of DME at the operating pressure of the column is 81 °C. As in the case of the COOLER, if no cooling water is available, the prefractionator side trim cooler condenser could be substituted by an air cooler exchanger resulting in a higher condensation temperature and therefore a lower recovery of DME in the column. Recycling more DME to the reaction zone will increase the CO₂ compressor power and decrease the equilibrium conversion in the hydrogenation reactor. The DWC has a dividing wall from the top of the column to the 12 tray and 10 additional trays located below the divided wall section. The bottom stream, with a minimum content of DME, is sent to the methanol-water distillation column (tray 21).

Finally, a second distillation column is used to separate methanol from water. This 33-stage column obtains high-purity methanol and water (>99.99 % mass). The column, operated at atmospheric pressure to minimize capital costs, uses air as a cooling fluid in the condenser.

The heat and material balance of the process is provided in Table 6, and the equipment sizing and main design parameters are provided in the *Supplementary Information* file.

4.2.2. Reactor technology selection

As explained in the previous section, an operating temperature of 250 °C is selected for the reactor as it provides a trade-off between the equilibrium conversion reached in the reactor and the amount of catalyst needed. An isothermal configuration is preferred over an adiabatic or a multitubed reactor since while the use of an adiabatic reactor would result in a lower equilibrium conversion and lower heat generation, the capital cost of a multitubed reactor with intercooling is higher. Although, to our knowledge, there are still no commercial reactors to hydrogenate CO₂ into a mixture of DME and methanol, the same industrial reactors used for methanol production (Casale, 2023; Topsoe, 2023; Linde, 2023) could be considered substituting the methanol synthesis catalyst by a combination of methanol synthesis catalyst and methanol dehydration catalyst. These isothermal reactors are cooled by circulating boiler feed water along the reactor absorbing the heat of the reaction and producing steam.

4.2.3. Dividing wall column design

The DWC presented in this work is divided into two sections: the upper divided section (trays along the dividing wall), and the lower common section (trays below the wall). The DWC is simulated using three rigorous distillation RADFRAC columns located in a subflowsheet of the simulation. Additional details on how a DWC is simulated can be found in Vaquerizo and Kiss (2023). The dividing wall column was simulated adjusting the boilup ratio and the main column reflux ratio to ensure a minimum DME purity of 99.99 % mass in the product stream without requiring any additional purification process, and a maximum DME content of 0.001 % mass in the DWC bottoms outlet stream. On the other hand, for the prefractionator side, the condenser outlet temperature was fixed at 40 °C. Finally, the number of trays of the divided section and the lower common section, and the vapor split ratio were optimized by the $N \times (RR+1)$ vs N plot (number of trays multiplied by reflux ratio plus 1 vs number of trays) and the reboiler duty vs vapor split ratio plot respectively, as shown in Figs. 5 and 6. The $N \times (RR+1)$ vs N plot combines both the capital cost of the column, as it includes the number of trays (N), with the operating costs, as it accounts for the reflux ratio ($RR+1$). For the upper-divided section, the optimum number of trays was fixed at 12 since, while in the prefractionator the $N \times (RR+1)$ vs N minimum is reached at 12–13 trays, in the main column the minimum is reached when 11–12 trays are used. On the other hand, for the lower common section, 10 trays were selected since, as shown in

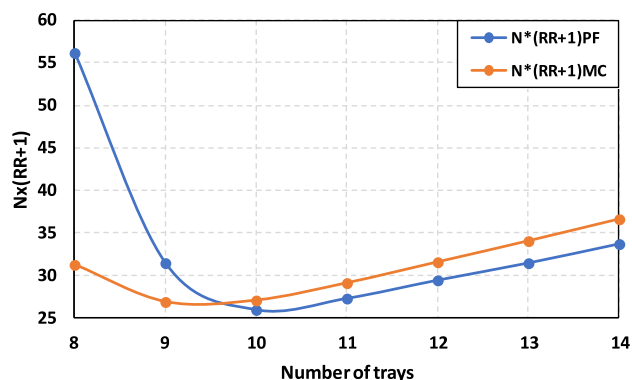
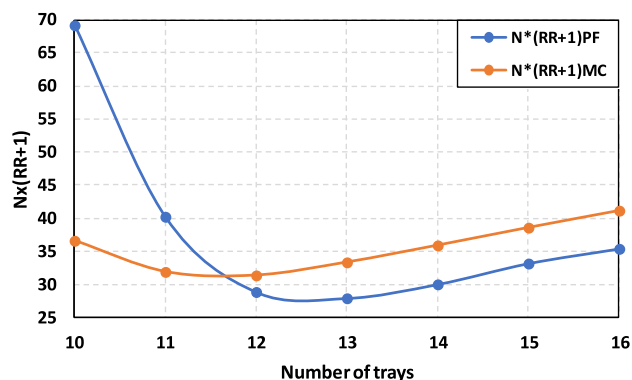


Fig. 5. Variation of $N \times (RR+1)$ with number of trays for the upper section (top) and for the lower section of the DWC (bottom).

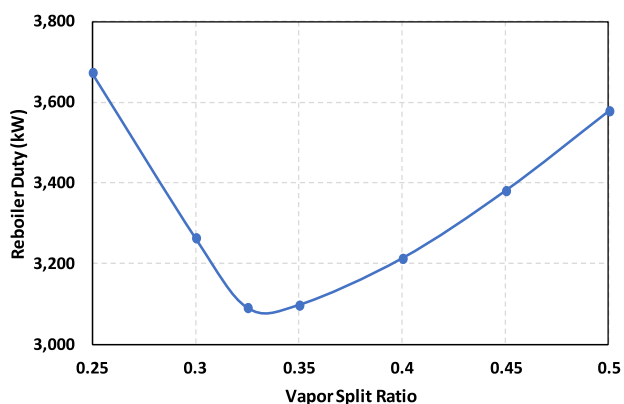


Fig. 6. Reboiler duty vs vapor split ratio for the DWC.

Fig. 5, while 9 trays optimize the main column section, 10 trays optimize the prefractionation section. Finally, as shown in Fig. 6, the DWC performance is optimized when 33 % of the vapor is sent to the prefractionation side. The temperature and composition profiles along the DWC are provided in Fig. 8.

4.2.4. Distillation column design

The last step in the design of the process is the optimization of the distillation column that separates methanol and water. The optimization is done again by using the $N \times (RR+1)$ vs N plot (Fig. 7), as it accounts for both the capital and the operating costs. The boilup and reflux ratios in the column are fixed to obtain minimum methanol and water purities of 99.99 % mass without needing any further purification process. The

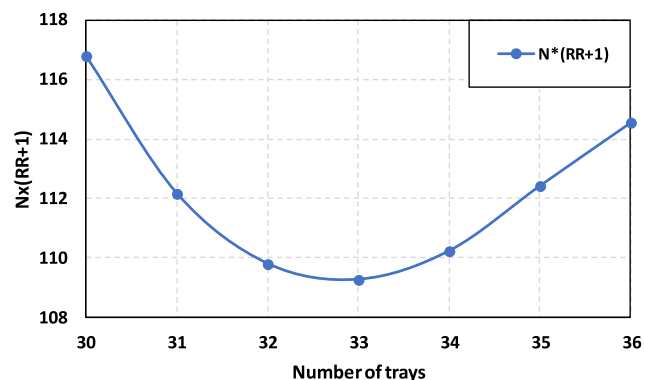


Fig. 7. Variation of $N \times (RR+1)$ with the number of trays for methanol-water distillation column.

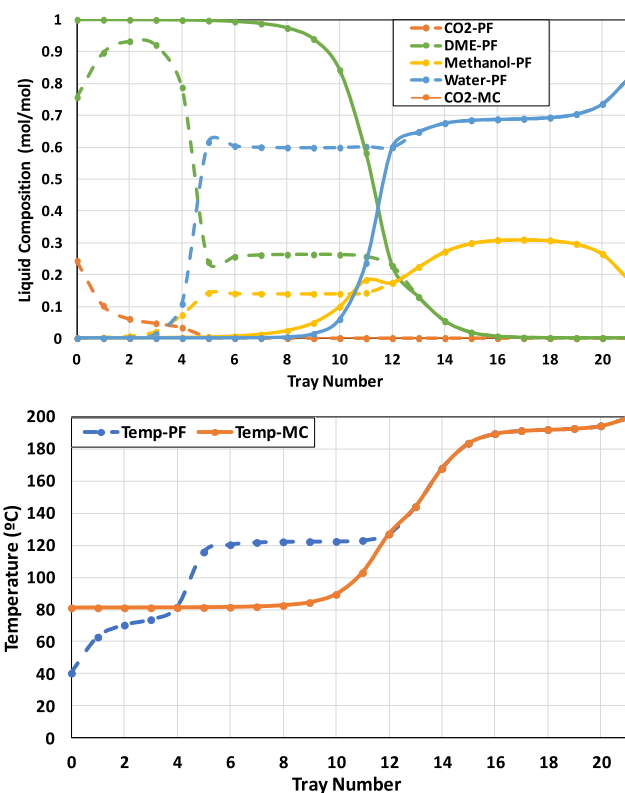


Fig. 8. Composition profiles (top) and temperature profiles (bottom) along the dividing-wall column.

optimum number of trays for this column is equal to 33.

4.3. Key parameters and consumption figures

Table 5 presents the key parameters and consumption figures of this process. This process converts CO₂ and H₂ into high-purity DME and methanol (>99.99 %wt) at almost maximum stoichiometric yield (99.97 %mol). The process is thermally self-sufficient (not requiring any external heat source) and uses only air and cooling water as cooling fluids. The reaction loop configuration, without any decompression valve in the loop, reduces the power consumption in the recycle compressor, as this compressor only needs to account for the pressure drop in the reaction circuit. In the case of the CO₂ and H₂ make-up compressors, since there is no generation of byproducts (apart from

Table 5

Key performance indicators for the proposed thermally self-sufficient process for DME and methanol coproduction by CO₂ hydrogenation.

| Parameter | Value | Unit |
|--|-------|------------------|
| MeOH production rate | 30.63 | kton/year |
| DME production rate | 49.84 | kton/year |
| Purge to feed ratio | 0 | mol/mol |
| Recycle to feed ratio | 2.71 | mol/mol |
| H ₂ :CO ₂ ratio (feed/reactor inlet) | 3/3 | mol/mol |
| H ₂ conversion in reactor (per pass) | 28.70 | % |
| CO ₂ conversion (per pass) | 28.76 | % |
| MeOH yield (overall process) | 30.64 | % |
| DME yield (overall process) | 69.33 | % |
| Products yield (overall process) | 99.97 | % |
| Power of H ₂ feed compressor | 5704 | kW |
| Power of CO ₂ feed compressor | 1860 | kW |
| Power of recycle compressor | 97 | kW |
| Electricity usage (per ton products) | 771 | kWh/ton products |
| Pure CO ₂ use (per unit of products) | 1.706 | kg/kg |
| Pure H ₂ use (per unit of products) | 0.234 | kg/kg |
| Wet H ₂ use (per unit of products) | 0.263 | kg/kg |

water), and there is no purge of reaction products (when no inerts are fed to the unit), the power consumption in these compressors is limited to the power required to compress the CO₂ and H₂ converted in the hydrogenation reactor.

The key operating parameters that mostly affect the performance of the plant are the operating pressure and temperature of the reactor. While a higher operating pressure in the reactor means a higher equilibrium conversion (Fig. 2) and higher compression requirements, higher operating temperatures result in lower equilibrium conversions (Figs. 2 and 3) and catalyst loads. An increase in the operating pressure of the reactor would therefore mean a higher conversion of the reagents into products and more heat generated in the reactor, but also higher costs related to the compression of the feed streams. Conversely, an increase in the reaction temperature would mean lower conversion of the reagents into products, lower heat generation, but also a decrease in the catalyst load and therefore in the reactor size.

The operating conditions of the process have been selected based on our previous work on methanol production by CO₂ hydrogenation Vaquerizo and Kiss (2023). However, the final operating conditions of the process will be selected to minimize the total annualized costs TAC (annualized capital costs + operating costs) and will mainly depend on the expected electricity cost and the required DME/methanol production ratio (fixed by the market demand). While a low electricity cost will allow for increasing the operating pressure in the reactor, increasing at the same time the conversion and heat generation and reducing the reactor volume and heat exchanger areas - see Vaquerizo and Kiss (2023) for more details - a high electricity cost will mean decreasing the reactor operating pressure to reduce the power consumption in the CO₂ and H₂ makeup compressors. Although higher operating pressures lead to higher conversions and heat generation in the reactor, better material and energetic efficiencies in the plant, and lower CAPEX and production costs, depending on the type of electricity used in the plant the environmental impact of the process will change. When green electricity is used, the much lower environmental impact of this type of electricity will benefit an increase in the operating pressure of the hydrogenation reactor improving the material and energetic efficiencies and reducing the production costs. However, when grey electricity is used, the higher environmental impact will lead to a reduction in the operating pressure of the reactor, meaning lower material and energetic efficiencies, and higher CAPEX and production costs. On the other hand, the DME/methanol production ratio can be adjusted by modifying the methanol production/methanol dehydration catalysts ratio, by recycling part of the methanol recovered in the distillation column to the hydrogenation reactor, or by including a reactive distillation column to convert methanol to DME (Bildea et al., 2017). While the first option does not provide flexibility during plant operation, the second and third options may

require an additional heat source due to the lower amount of heat released in the reactor and the duty required in the reboiler of the reactive distillation column. Once the desired DME/methanol production ratio is selected, the process parameters will be dynamically optimized to minimize the production cost and environmental impact, while ensuring the safe operation of the plant. As explained earlier in this section, the efficiency of the plant, the environmental impact, and the production costs are interconnected parameters. The operating pressure in the reactor is adjusted depending on the electricity cost and whether green or grey electricity is used. When green electricity is used, the control system of the plant will raise the operating pressure in the hydrogenation reactor to increase the equilibrium conversion, and the overall process yield, optimizing the production costs. On the other hand, when grey electricity, with a higher environmental impact, is used, or in high electricity cost scenarios, the control system of the plant will act reducing the operating pressure of the hydrogenation reaction, minimizing the electricity consumption, the production cost, and the environmental impact. If any impurities are present in the CO₂ stream, the control system will act by dynamically tracking the pressure in the reaction loop and opening a control valve located in the purge line to avoid the accumulation of impurities and pressure buildup while ensuring minimum purging of products. Finally, if there is a change in the production scheme requiring a higher amount of DME, the control system will act by increasing the operating pressure in the hydrogenation reactor to generate some extra heat that can cover the additional heat necessities related to DME production. In the same way, the control systems located in the dividing wall column and the distillation column will act to minimize the duty provided in both columns while maintaining the required product specifications.

Finally, the H₂ and CO₂ production prices will affect the minimum selling price of the products determining whether this production route can compete with the conventional methanol and DME production processes.

4.4. Sustainability metrics

The sustainability of the process was evaluated using several indicators proposed by Sheldon (2018) and Dicks and Hent (2015), where lower values of these metrics represent a better performance of the process in terms of sustainability. Compared with previously published works, this process results in a cleaner methanol and DME production route because there is no waste of raw materials, the process is thermally self-sufficient, so there is no consumption of external fuels, and the GHG emissions are only limited to those required to produce hydrogen and CO₂, yielding methanol and DME at practically 100 % rate, and to those required in the production of green electricity, with the lowest consumption rate per ton of produced methanol and DME. Regarding the potential by-products of the process, they are limited to the spent solid catalyst of the hydrogenation reactor, which will be disposed of following all the environmental regulations being regenerated by the catalyst supplier and reused in the process, to the water stream recovered at the bottoms of the distillation column, which contains traces of methanol and that will be sent to a wastewater treatment plant, and the greenhouse gas emissions related to the production of electricity, especially when grey electricity is used in the plant. As for the potential by-products of the process, they are limited to the spent solid catalyst of the hydrogenation reactor, which will be disposed of following all the environmental regulations being regenerated by the catalyst supplier and reused in the process, to the water stream recovered at the bottoms of the distillation column, which contains traces of methanol and that will be sent to a wastewater treatment plant, and the greenhouse gas emissions related to the production of electricity, especially when grey electricity is used in the plant. As the process uses a CO₂-based feed gas the yield of byproducts formation remains below 0.05 %wt (Dieterich et al., 2020) and no special handling and disposal treatment is needed.

Table 6
Mass and energy balance of the proposed process.

| | F-CO ₂ | CO ₂ -HP | CO ₂ -R | F-H ₂ | H ₂ -HP | WATER-C | R-2 | F-1 | F-2 | F-3 | P-1 | P-2 | P-3 | P-4 | P-5 |
|---------------------------|-------------------|---------------------|--------------------|------------------|--------------------|---------|---------|---------|---------|---------|---------|---------|---------|---------|---------|
| Temperature (°C) | 25.0 | 163.4 | 50.2 | 35.0 | 175.0 | 55.4 | 42.3 | 71.7 | 177.0 | 220.0 | 250.0 | 156.3 | 140.6 | 129.2 | 40.0 |
| Pressure (bara) | 1.0 | 65.0 | 23.0 | 1.1 | 65.0 | 12.7 | 65.0 | 65.0 | 64.9 | 64.7 | 64.1 | 64.0 | 63.8 | 63.7 | 63.5 |
| Vapor frac (mol/mol) | 1 | 1.00 | 1.00 | 1.00 | 1.00 | 0.00 | 1.00 | 1.00 | 1.00 | 1.00 | 1.00 | 1.00 | 0.96 | 0.94 | 0.83 |
| Mole flow (kmol/h) | 390.0 | 431.7 | 41.7 | 1186.1 | 1177.3 | 8.7 | 4214.0 | 5837.3 | 5837.3 | 5837.3 | 5057.3 | 5057.3 | 5057.3 | 5057.3 | 5057.3 |
| Mass flow (kg/h) | 17,164 | 18,933 | 1769 | 2650 | 2492 | 158 | 62,988 | 84,930 | 84,930 | 84,929 | 84,929 | 84,929 | 84,929 | 84,929 | 84,929 |
| Volume flow (cum/h) | 9620 | 225 | 41 | 27,642 | 695 | 0 | 1665 | 2534 | 3328 | 3675 | 3370 | 2684 | 2509 | 2398 | 1723 |
| Enthalpy (gcal/h) | −36.72 | −39.10 | −2.83 | −0.85 | 0.82 | −0.59 | −103.46 | −142.56 | −137.79 | −135.53 | −140.48 | −145.25 | −147.21 | −148.79 | −157.11 |
| Mass frac CO ₂ | 1.0000 | 0.9572 | 0.5418 | 0.0000 | 0.0000 | 0.0000 | 0.6553 | 0.7026 | 0.7026 | 0.7026 | 0.5005 | 0.5005 | 0.5005 | 0.5005 | 0.5005 |
| Mass frac H ₂ | 0.0000 | 0.0002 | 0.0026 | 0.8900 | 0.9463 | 0.0000 | 0.0929 | 0.0968 | 0.0968 | 0.0968 | 0.0690 | 0.0690 | 0.0690 | 0.0690 | 0.0690 |
| Mass frac CO | 0.0000 | 0.0001 | 0.0009 | 0.0000 | 0.0000 | 0.0000 | 0.0263 | 0.0195 | 0.0195 | 0.0195 | 0.0195 | 0.0195 | 0.0195 | 0.0195 | 0.0195 |
| Mass frac DME | 0.0000 | 0.0421 | 0.4502 | 0.0000 | 0.0000 | 0.0000 | 0.2197 | 0.1749 | 0.1749 | 0.1749 | 0.2482 | 0.2482 | 0.2482 | 0.2482 | 0.2482 |
| Mass frac METHANOL | 0.0000 | 0.0003 | 0.0035 | 0.0000 | 0.0000 | 0.0000 | 0.0036 | 0.0029 | 0.0029 | 0.0029 | 0.0480 | 0.0480 | 0.0480 | 0.0480 | 0.0480 |
| Mass frac WATER | 0.0000 | 0.0001 | 0.0010 | 0.1100 | 0.0537 | 1.0000 | 0.0022 | 0.0034 | 0.0034 | 0.0034 | 0.1148 | 0.1148 | 0.1148 | 0.1148 | 0.1148 |
| Mole frac CO ₂ | 1.0000 | 0.9539 | 0.5226 | 0.0000 | 0.0000 | 0.0000 | 0.2226 | 0.2323 | 0.2323 | 0.2323 | 0.1910 | 0.1910 | 0.1910 | 0.1910 | 0.1910 |
| Mole frac H ₂ | 0.0000 | 0.0052 | 0.0542 | 0.9864 | 0.9937 | 0.0004 | 0.6886 | 0.6983 | 0.6983 | 0.6983 | 0.5747 | 0.5747 | 0.5747 | 0.5747 | 0.5747 |
| Mole frac CO | 0.0000 | 0.0001 | 0.0013 | 0.0000 | 0.0000 | 0.0000 | 0.0140 | 0.0102 | 0.0102 | 0.0102 | 0.0117 | 0.0117 | 0.0117 | 0.0117 | 0.0117 |
| Mole frac DME | 0.0000 | 0.0400 | 0.4148 | 0.0000 | 0.0000 | 0.0000 | 0.0713 | 0.0552 | 0.0552 | 0.0552 | 0.0905 | 0.0905 | 0.0905 | 0.0905 | 0.0905 |
| Mole frac METHANOL | 0.0000 | 0.0005 | 0.0047 | 0.0000 | 0.0000 | 0.0000 | 0.0017 | 0.0013 | 0.0013 | 0.0013 | 0.0251 | 0.0251 | 0.0251 | 0.0251 | 0.0251 |
| Mole frac WATER | 0.0000 | 0.0002 | 0.0023 | 0.0136 | 0.0063 | 0.9996 | 0.0018 | 0.0027 | 0.0027 | 0.0027 | 0.1070 | 0.1070 | 0.1070 | 0.1070 | 0.1070 |
| | R-1 | PURGE | P-6 | P-7 | FR-1 | P-8 | P-9 | P-10 | FR-2 | P-11 | R-3 | DME | HEAVIES | MEOH | WATER |
| Temperature (°C) | 40.0 | 40.0 | 40.1 | 122.0 | 122.0 | 122.0 | 111.6 | 111.6 | 55.0 | 55.0 | 40.4 | 81.0 | 199.1 | 66.6 | 107.5 |
| Pressure (bara) | 63.5 | 63.5 | 65.0 | 65.0 | 65.0 | 65.0 | 23.2 | 23.2 | 23.2 | 23.2 | 23.0 | 23.0 | 23.1 | 1.1 | 1.3 |
| Vapor frac (mol/mol) | 1.00 | 1.0 | 0.00 | 0.02 | 1.00 | 0.00 | 0.00 | 1.00 | 1.00 | 0.00 | 1.00 | 0.00 | 0.00 | 0.00 | 0.00 |
| Mole flow (kmol/h) | 4214.0 | 0.0 | 843.3 | 843.3 | 14.3 | 829.0 | 765.5 | 63.5 | 27.7 | 35.8 | 14.0 | 135.2 | 652.1 | 119.5 | 532.7 |
| Mass flow (kg/h) | 62,989 | 0 | 21,940 | 21,940 | 516 | 21,424 | 18,794 | 2630 | 1149 | 1481 | 620 | 6230 | 13,425 | 3829 | 9596 |
| Volume flow (cum/h) | 1692 | 0 | 31 | 40 | 6 | 34 | 29 | 76 | 28 | 2 | 13 | 13 | 24 | 7 | 14 |
| Enthalpy (gcal/h) | −103.54 | 0.00 | −53.57 | −51.99 | −0.83 | −51.16 | −47.57 | −3.59 | −1.78 | −2.04 | −1.05 | −6.37 | −40.98 | −6.74 | −35.64 |
| Mass frac CO ₂ | 0.6553 | 0.6553 | 0.0560 | 0.0560 | 0.5228 | 0.0447 | 0.0104 | 0.2899 | 0.5010 | 0.1261 | 0.6175 | 0.0000 | 0.0000 | 0.0000 | 0.0000 |
| Mass frac H ₂ | 0.0929 | 0.0929 | 0.0004 | 0.0004 | 0.0090 | 0.0002 | 0.0000 | 0.0017 | 0.0037 | 0.0001 | 0.0005 | 0.0000 | 0.0000 | 0.0000 | 0.0000 |
| Mass frac CO | 0.0263 | 0.0263 | 0.0002 | 0.0002 | 0.0036 | 0.0001 | 0.0000 | 0.0006 | 0.0013 | 0.0000 | 0.0002 | 0.0000 | 0.0000 | 0.0000 | 0.0000 |
| Mass frac DME | 0.2197 | 0.2197 | 0.3300 | 0.3300 | 0.4147 | 0.3280 | 0.2843 | 0.6400 | 0.4871 | 0.7586 | 0.3819 | 1.0000 | 0.0000 | 0.0000 | 0.0000 |
| Mass frac METHANOL | 0.0036 | 0.0036 | 0.1754 | 0.1754 | 0.0262 | 0.1790 | 0.1987 | 0.0384 | 0.0054 | 0.0639 | 0.0000 | 0.0000 | 0.2852 | 0.9999 | 0.0001 |
| Mass frac WATER | 0.0022 | 0.0022 | 0.4380 | 0.4380 | 0.0237 | 0.4480 | 0.5065 | 0.0296 | 0.0015 | 0.0513 | 0.0000 | 0.0000 | 0.7148 | 0.0001 | 0.9999 |
| Mole frac CO ₂ | 0.2226 | 0.2226 | 0.0331 | 0.0331 | 0.4304 | 0.0263 | 0.0058 | 0.2726 | 0.4725 | 0.1183 | 0.6218 | 0.0000 | 0.0000 | 0.0000 | 0.0000 |
| Mole frac H ₂ | 0.6886 | 0.6886 | 0.0054 | 0.0054 | 0.1615 | 0.0027 | 0.0001 | 0.0340 | 0.0763 | 0.0013 | 0.0105 | 0.0000 | 0.0000 | 0.0000 | 0.0000 |
| Mole frac CO | 0.0140 | 0.0140 | 0.0001 | 0.0001 | 0.0046 | 0.0001 | 0.0000 | 0.0008 | 0.0019 | 0.0000 | 0.0003 | 0.0000 | 0.0000 | 0.0000 | 0.0000 |
| Mole frac DME | 0.0713 | 0.0713 | 0.1864 | 0.1864 | 0.3261 | 0.1840 | 0.1515 | 0.5750 | 0.4388 | 0.6803 | 0.3674 | 1.0000 | 0.0000 | 0.0000 | 0.0000 |
| Mole frac METHANOL | 0.0017 | 0.0017 | 0.1424 | 0.1424 | 0.0297 | 0.1444 | 0.1522 | 0.0496 | 0.0070 | 0.0824 | 0.0000 | 0.0000 | 0.1832 | 0.9999 | 0.0000 |
| Mole frac WATER | 0.0018 | 0.0018 | 0.6325 | 0.6325 | 0.0477 | 0.6426 | 0.6903 | 0.0679 | 0.0035 | 0.1177 | 0.0000 | 0.0000 | 0.8168 | 0.0001 | 1.0000 |

- **Material intensity.** This parameter quantifies the total amount of raw materials required for producing a unit of product. In this process, the material intensity is equal to 1.94 kg raw materials/kg products, since 19,523 kg/h of CO₂ and H₂ are required to produce 10,059 kg/h of products (DME & methanol). Compared with previously published works on DME production by CO₂ hydrogenation, this process requires less CO₂ and H₂ to produce the products. While the material intensity in the process published by Poto et al. (2023) is 2.18 kg raw materials/kg products, in the process of Michailos et al. (2019) the material intensity is 2.30 kg raw materials/kg products.
- **E-factor** quantifies the amount of waste produced in the process per kg of products. In this process, water is considered a by-product of the CO₂ hydrogenation reaction as part of the CO₂ fed to the unit ends up converted into water (9462 kg/h) instead of into DME (6230 kg/h) or methanol (3829 kg/h). The resulting E-factor for this process is equal to 0.94 kg water/kg product.
- **Energy intensity** measures the total amount of energy that is consumed per kilogram of products. For energy intensity calculation, since the process is thermally self-sufficient, the energy intensity is calculated as the power consumption required in the CO₂, recycling, and hydrogen compressors divided by the sum of the DME and methanol production. The compressors of this DME-methanol production plant consume 7661 kW to compress the CO₂ and H₂ required in the production of 6230 kg/h of DME and 3829 kg/h of methanol. Thus, the resulting energy intensity is 0.76 kWh_e/kg_{products} (2.74 MJ/kg_{products}). When grey electricity is used instead of green, considering that 2.5 units of primary energy are required to produce 1 unit of electricity, the equivalent primary energy requirements are 1.90 kWh_{th}/kg_{products}. The value of the energy intensity will fluctuate between 0.76 kWh_e/kg_{products} and 1.90 kWh_{th}/kg_{products} depending on the source of power used in the plant. Compared with previously published works on DME production by CO₂ hydrogenation, this process achieves a reduction in the amount of energy required per kilogram of DME. The process presented by Poto et al. (2023) consumed 967 kWe to produce 1369 kg/h of DME (energy intensity of 0.71 kWh_e/kg_{DME}). On the other hand, Michailos et al. (2019) reported an energy consumption of 0.904 kWh_e/kg_{DME}. To be able to compare the energy intensity of this process with previously published processes, for the hydrogen compressor, only the power consumption of the last stage (compression from 29 bar to 65 bar) is considered since the electrical consumptions reported by both Poto et al. (2023) and Michailos et al. (2019) were based on an H₂ supply pressure of 35 bar. In this way, the resulting energy intensity of the process is equal to 0.49 kWh_e/kg_{DME} (the previously reported energy intensity of 0.76 kWh_e/kg_{products} accounted for the H₂ compression to 65 bar from a supply pressure of 1 bar).
- **Water consumption.** This sustainability indicator is used to account for the total amount of freshwater consumed in the process per kilogram of products. Although in this process water is recovered in the interstage KO drums of the H₂ compressor and at the bottoms of the methanol-water distillation column, for the calculation of this sustainability metric it has been considered that this water is not reused in the process. Thus, the water consumption is only related to the cooling water losses in the cooling tower of the plant. Assuming a typical loss of 7 % of cooling water in the cooling water tower, that cooling water is only used in the condenser of the DWC pre-fractionator and the cooler, and a maximum temperature change for cooling water in the cooling water heat exchangers of 10 °C, 60 m³/h of water are lost in the process. The water consumption in the process is therefore equal to 0.006 m³_{water}/kg_{products}. This figure can be reduced even further if the cooler is substituted by a combination of an air cooler and a cooling water heat exchanger. The environmental feasibility of substituting the cooler with a combination of an air cooler and a cooling water exchanger will depend on the power source. If green electricity is used in the plant, the use of an air cooler will be more environmentally attractive. However, if grey electricity

is used, the CO₂ emissions related to the production of grey electricity will penalize the environmental sustainability of this alternative. From an economic point of view, it has to be considered that when using cooling water as a cooling fluid, the heat transfer coefficient of the cold side is higher than with air, meaning a reduction in the heat exchanger area and capital cost of the equipment. Compared with previously published works on DME production by CO₂ hydrogenation, this process achieves a reduction in water consumption (0.006 m³_{water}/kg_{products} or 0.010 m³_{water}/kg_{DME}). While in the process proposed by Poto et al. (2023), the cooling water circulation was 260 t/h for a DME production of 1369 kg/h, meaning a water consumption of 0.013 m³_{water}/kg_{DME} (considering also 7 % of cooling water loss), in the work published by Michailos et al. (2019), the cooling water circulation increased up to 6426 t/h for a DME production of 30.7 t/h, meaning a water consumption of 0.015 m³_{water}/kg_{DME}.

- **Greenhouse gas (GHG) emissions.** The greenhouse gas (GHG) emissions of this process are related to the electricity required in the compressors of the plant, the production of hydrogen consumed in the reactor, and the capture of CO₂ used as raw material. For the calculation of this metric, two different scenarios have been considered (green electricity and hydrogen/grey electricity and hydrogen). In the first one, based on operating using green electricity and green hydrogen (hydrogen produced by water electrolysis using wind as the power source), the total CO_{2eq} emissions are equal to 0.50 kgCO_{2eq}/kg_{products}. In the second one, based on grey electricity (electricity produced from fossil fuels) and grey hydrogen (hydrogen produced by steam reforming of natural gas without carbon capture), the CO₂ emissions increase up to 2.35 kgCO_{2eq}/kg_{products}. Since 17,164 kg of CO₂ are consumed every hour, the net CO_{2eq} emissions decrease to -1.20 kgCO_{2eq}/kg_{products} using green hydrogen and electricity and to 0.64 kgCO_{2eq}/kg_{products} using grey hydrogen and electricity. Additional details can be found in the *Supplementary Information* file. The GHG emissions of this process are lower than the ones of the processes published by Poto et al. (2023) and Michailos et al. (2019) since the material intensity is lower (fewer emissions related to the production of raw materials), the energy intensity is also lower (fewer emissions related to power production), and both the process of Poto et al. (2023) and Michailos et al. (2019) were not thermally self-sufficient and consumed natural gas.

The sustainability of the process is also supported by the fact that the CO₂ fed to the unit is converted at maximum yield into DME and methanol, the only byproduct of the process is water, and the process is thermally self-sufficient not requiring the usage of an external fuel (as illustrated by the composite curves shown in Fig. 9).

5. Conclusions

This work proposed and successfully demonstrated a novel thermally self-sufficient process for the coproduction of DME and methanol in a single-step reactor. The main outcomes of this study are as follows.

- The DME-synthesis reaction is performed in an isothermal catalytic reactor that operates at 250 °C containing a mixture of catalysts (Cu/Zn/Al/Zr & H-FER 20) for methanol synthesis and dehydration. This reaction temperature balances the equilibrium conversion with the amount of catalyst needed in the reactor. When operating at a GHSV of 1.5 m³/kg_{cat}·h, the reaction is equilibrium limited and provides sufficient heat to cover all the heat necessities of the process. The selection of the operating pressure depends on the electricity cost. Low electricity prices favor an increase in the operating pressure (up to a certain limit determined by the equipment thicknesses) as it reduces the reactor recycling stream and increases the LMTD in the heat exchangers of the plant. On the other hand, with a high

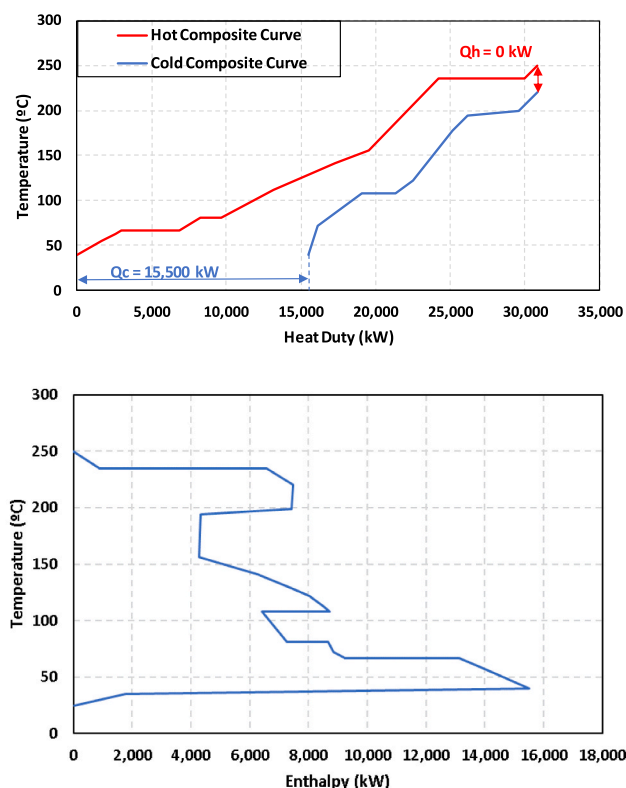


Fig. 9. Hot and cold composite curves (upper graph) and Grand Composite Curve (lower graph) of a thermally self-sufficient process for DME and methanol coproduction by CO₂ hydrogenation.

electricity prices perspective, lower operating pressures are preferred (because of the reduction in the compressors' power).

- The top divided wall column used in the process can recover all the unreacted CO₂ and obtained a purified DME stream (>99.99 % mass). The operating pressure of the column is balanced with the outlet of the third stage of the CO₂ compressor allowing for a lower DME recycling and a reduction in the CO₂ compressor power.
- Limiting the pressure loss in the reaction-separation-recycle loop to the hydraulic pressure drop (no expansion valve used in this section) decreased the power consumption to 0.76 kWh per kg products.
- The process only produces water as a byproduct (0.94 kg_{water}/kg_{products}) and does not consume any external fuel or refrigerant, only cooling water at 0.006 m³_{water}/kg_{products} and electricity (0.76 kWh_e/kg_{products}). The net GHG emissions are limited to −1.20 or 0.64 kgCO_{2eq}/kg_{products} when green or grey electricity are used, respectively.
- The main two limitations of the process are the fact that an external heat source is needed during the startup of the plant to reach the reaction temperature and that a backup power source is needed if it is not possible to ensure a stable supply of green electricity to the plant.

CRedit authorship contribution statement

Luis Vaquerizo: Writing – original draft, Writing – review & editing, Visualization, Validation, Resources, Methodology, Investigation, Formal analysis, Conceptualization. **Anton A. Kiss:** Writing – original draft, Writing – review & editing, Visualization, Validation, Supervision, Resources, Project administration, Methodology, Investigation, Formal analysis, Conceptualization.

Declaration of competing interest

The authors declare that they have no known competing financial interests or personal relationships that could have appeared to influence the work reported in this paper.

Data availability

Data will be made available on request.

Acknowledgment

Luis Vaquerizo thanks the Spanish Ministry of Universities for the mobility funding (Estancias de Movilidad en el extranjero José Castillejo para jóvenes doctores).

Appendix A. Supplementary data

Supplementary data to this article can be found online at <https://doi.org/10.1016/j.jclepro.2024.140949>.

References

- Aguayo, A.T., Erená, J., Mier, D., Arandes, J.M., Olazar, M., Bilbao, J., 2007. Kinetic modeling of dimethyl ether synthesis in a single step on a CuO-ZnO-Al₂O₃/γ-Al₂O₃ catalyst. *Ind. Eng. Chem. Res.* 46, 5522–5530. <https://doi.org/10.1021/ie070269s>.
- An, X., Zuo, Y., Zhang, Q., Wang, J., 2009. Methanol synthesis from CO₂ hydrogenation with a Cu/Zn/Al/Zr fibrous catalyst. *Chin. J. Chem. Eng.* 17, 88–94. [https://doi.org/10.1016/S1004-9541\(09\)60038-0](https://doi.org/10.1016/S1004-9541(09)60038-0).
- Azizi, Z., Rezaeimanesh, M., Tohidian, T., Rahimpour, M.R., 2014. Dimethyl ether: a review of technologies and production challenges. *Chem. Eng. Process: Process Intensif.* 82, 150–172. <https://doi.org/10.1016/j.cep.2014.06.007>.
- Banivahab, S., Pitter, S., Delgado, K.H., Rubin, M., Sauer, J., Dittmeyer, R., 2022. Recent progress in direct DME synthesis and potential of bifunctional catalysts. *Chem.-Ing.-Tech.* 94 (3), 240–255. <https://doi.org/10.1002/cite.202100167>.
- Bildea, C.S., György, R., Brunchi, C.C., Kiss, A.A., 2017. Optimal design of intensified processes for DME synthesis. *Comput. Chem. Eng.* 105, 142–151. <https://doi.org/10.1016/j.compchemeng.2017.01.004>.
- Casale, 2023. <https://www.casale.ch/technologies/methanol-synthesis-reactor>. (Accessed 9 November 2023) [WWW Document].
- Diban, N., Urtiaga, A.M., Ortiz, I., Erená, J., Bilbao, J., Aguayo, A.T., 2014. Improved performance of a PBM reactor for simultaneous CO₂ capture and DME synthesis. *Ind. Eng. Chem. Res.* 53 (50), 19479–19487. <https://doi.org/10.1021/ie503663h>.
- Dicks, A.P., Hent, A., 2015. Green chemistry for sustainability green chemistry metrics A guide to determining and evaluating process greenness. In: Sharma, S.K. (Ed.), *Springer Briefs in Molecular Science*, first ed. <https://doi.org/10.1007/978-3-319-10500-0>.
- Dieterich, V., Buttler, A., Hanel, A., Spliethoff, H., Fendt, S., 2020. Power-to-liquid via synthesis of methanol, DME or Fischer-Tropsch fuels: a review. *Energy Environ. Sci.* 13 (3) <https://doi.org/10.1039/d0ee01187h>, 207–3,252.
- Dikić, V., Zubeir, L., Sarić, M., Boon, J., 2023. Stripping enhanced distillation—a novel application in renewable CO₂ to dimethyl ether production and purification. *Separations* 10, 403. <https://doi.org/10.3390/separations10070403>.
- Dimian, A.C., Bildea, C.S., Kiss, A.A., 2019. *Applications in Design and Simulation of Sustainable Chemical Processes*. Elsevier, The Netherlands.
- Fiedler, E., Grossmann, G., Kersebohm, D., Weiss, G., Witte, C., 2005. Methanol. In: *Ullmann's Encyclopedia of Industrial Chemistry*. Wiley-VCH.
- Fleisch, T., Basu, A., Gradasi, M.J., Masin, J.G., 1997. Dimethyl ether: a fuel for the 21st century. *Stud. Surf. Sci. Catal.* 107, 117–125. [https://doi.org/10.1016/S0167-2991\(97\)80323-0](https://doi.org/10.1016/S0167-2991(97)80323-0).
- Giampaolo, T., 2010. *Compressor Handbook Principles and Practices*. The Fairmont Press.
- Gor, N.K., Mali, N.A., Joshi, S.S., 2020. Intensified reactive distillation configurations for production of dimethyl ether. *Chemical Engineering and Processing - Process Intensification* 149, 107824. <https://doi.org/10.1016/j.cep.2020.107824>.
- Graaf, G.H., Sijtsma, P.J.J.M., Stamhuis, E.J., Joostes, G.E.H., 1986. Chemical equilibria in methanol synthesis. *Chem. Eng. Sci.* 41 (2) [https://doi.org/10.1016/0009-2509\(86\)80019-7](https://doi.org/10.1016/0009-2509(86)80019-7), 993–2,890.
- Graaf, G.H., Stamhuis, E.J., Beenackers, A.A.C.M., 1988. Kinetics of low-pressure methanol synthesis. *Chem. Eng. Sci.* 43 (3) [https://doi.org/10.1016/0009-2509\(88\)85127-3](https://doi.org/10.1016/0009-2509(88)85127-3), 185–3,195.
- Hassanpouryouzband, A., Adie, K., Cowen, T., Thaysen, E.M., Heinemann, N., Butler, I. B., Wilkinson, M., Edlmann, K., 2022. Geological hydrogen storage: geochemical reactivity of hydrogen with sandstone reservoirs. *ACS Energy Lett.* 7, 2203–2210. <https://doi.org/10.1021/acscenergylett.2c01024>.
- Hassanpouryouzband, A., Joonaki, E., Edlmann, K., Haszeldine, R.S., 2021. Offshore geological storage of hydrogen: is this our best option to achieve net-zero? *ACS Energy Lett.* 6, 2181–2186. <https://doi.org/10.1021/acscenergylett.1c00845>.

- Hassanpouryouzband, A., Joonaki, E., Vashghani Farahani, M., Takeya, S., Ruppel, C., Yang, J., English, N.J., Schicks, J.M., Edlmann, K., Mehrabian, H., Aman, Z.M., Tohidi, B., 2020. Gas hydrates in sustainable chemistry. *Chem. Soc. Rev.* 49, 5225–5309. <https://doi.org/10.1039/c8cs00989a>.
- Kanuri, S., Roy, S., Chakraborty, C., Datta, S.P., Singh, S.A., Dinda, S., 2022. An insight of CO₂ hydrogenation to methanol synthesis: thermodynamics, catalysts, operating parameters, and reaction mechanism. *Int. J. Energy Res.* 46 (5) <https://doi.org/10.1002/er.7562>, 503–505, 522.
- Kiss, A.A., Suszwalak, D.J.P.C., 2012. Innovative dimethyl ether synthesis in a reactive dividing-wall column. *Comput. Chem. Eng.* 38, 74–81. <https://doi.org/10.1016/j.compchemeng.2011.11.012>.
- Kiss, A.A., Pragt, J.J., Vos, H.J., Bargeman, G., de Groot, M.T., 2016. Novel efficient process for methanol synthesis by CO₂ hydrogenation. *Chem. Eng. J.* 284, 260–269. <https://doi.org/10.1016/j.cej.2015.08.101>.
- Lee, B., Lee, H., Lim, D., Brigljević, B., Cho, W., Cho, H.S., Kim, C.H., Lim, H., 2020. Renewable methanol synthesis from renewable H₂ and captured CO₂: how can power-to-liquid technology be economically feasible? *Appl. Energy* 279 (115), 827. <https://doi.org/10.1016/j.apenergy.2020.115827>.
- Lei, Z., Zou, Z., Dai, C., Li, Q., Chen, B., 2011. Synthesis of dimethyl ether (DME) by catalytic distillation. *Chem. Eng. Sci.* 66 (3) <https://doi.org/10.1016/j.ces.2011.02.034>, 195–3, 203.
- Leung, D., Caramanna, G., Maroto-Valer, M., 2014. An overview of current status of carbon dioxide capture and storage technologies. *Renew. Sustain. Energy Rev.* 39, 426–443. <https://doi.org/10.1016/j.rser.2014.07.093>.
- Linde, 2023. In: https://www.linde-engineering.com/en/process-plants/hydrogen_and_synthesis_gas_plants/gas_products/methanol/index.html. (Accessed 9 November 2023) [WWW Document].
- Lim, H.W., Park, M.J., Kang, S.H., Chae, H.J., Bae, J.W., Jun, K.W., 2009. Modeling of the kinetics for methanol synthesis using Cu/ZnO/Al₂O₃/ZrO₂ catalyst: influence of carbon dioxide during hydrogenation. *Ind. Eng. Chem. Res.* 48, 10448–10455. <https://doi.org/10.1021/ie901081f>.
- Lotfollahzade Moghaddam, A., Hazlett, M.J., 2023. Methanol dehydration catalysts in direct and indirect dimethyl ether (DME) production and the beneficial role of DME in energy supply and environmental pollution. *J. Environ. Chem. Eng.* 11, 110307. <https://doi.org/10.1016/j.jece.2023.110307>.
- Luyben, W.L., 2017. Improving the conventional reactor/separation/recycle DME process. *Comput. Chem. Eng.* 106, 17–22. <https://doi.org/10.1016/j.compchemeng.2017.05.008>.
- Michailos, S., McCord, S., Sick, V., Stokes, G., Styring, P., 2019. Dimethyl ether synthesis via captured CO₂ hydrogenation within the power to liquids concept: a techno-economic assessment. *Energy Convers. Manag.* 184, 262–276. <https://doi.org/10.1016/j.enconman.2019.01.046>.
- Müller, M., Hübsch, U., 2000. Dimethyl ether. In: Ullmann's Encyclopedia of Industrial Chemistry. Wiley-VCH Verlag GmbH & Co. KGaA, Weinheim, Germany. https://doi.org/10.1002/14356007.a08_541.
- Olah, G.A., Goeppert, A., Prakash, G.K.S., 2009. Chemical recycling of carbon dioxide to methanol and dimethyl ether: from greenhouse gas to renewable, environmentally carbon neutral fuels and synthetic hydrocarbons. *J. Org. Chem.* 74 (2), 487–498. <https://doi.org/10.1021/jo801260f>.
- Peinado, C., Liuzzi, D., Sluijter, S.N., Skorikova, G., Boon, J., Guffanti, S., Groppi, G., Rojas, S., 2024. Review and perspective: next generation DME synthesis technologies for the energy transition. *Chem. Eng. J.* 479, 147494. <https://doi.org/10.1016/j.cej.2023.147494>.
- Poto, S., Vink, T., Oliver, P., Gallucci, F., Neira D'angelo, M.F., 2023. Techno-economic assessment of the one-step CO₂ conversion to dimethyl ether in a membrane-assisted process. *J. CO₂ Util.* 69, 102419. <https://doi.org/10.1016/j.jcou.2023.102419>.
- Sheldon, R.A., 2018. Metrics of green chemistry and sustainability: past, present, and future. *ACS Sustain. Chem. Eng.* 6 (1), 32–48. <https://doi.org/10.1021/acssuschemeng.7b03505>.
- Topsoe, 2023. In: <https://www.topsoe.com/processes/methanol/synthesis>. (Accessed 9 November 2023) [WWW Document].
- Turton, R., Baille, R.C., Whiting, W.B., Shaelwitz, J.A., 2003. *Analysis, Synthesis and Design of Chemical Processes*, second ed. Prentice Hall, p. 939.
- Vaquerizo, L., Kiss, A.A., 2023. Thermally self-sufficient process for cleaner production of e-methanol by CO₂ hydrogenation. *J. Clean. Prod.* 433, 139845. <https://doi.org/10.1016/j.jclepro.2023.139845>.
- Vu, T.T.N., Desgagnés, A., Iliuta, M.C., 2021. Efficient approaches to overcome challenges in material development for conventional and intensified CO₂ catalytic hydrogenation to CO, methanol, and DME. *Appl. Catal. Gen.* 617, 118119. <https://doi.org/10.1016/j.apcata.2021.118119>.
- Wild, S., Lacerda de Oliveira Campos, B., Zevaco, T.A., Guse, D., Kind, M., Pitter, S., Herrera Delgado, K., Sauer, J., 2022. Experimental investigations and model-based optimization of CZZ/H-FER 20 bed compositions for the direct synthesis of DME from CO₂-rich syngas. *React. Chem. Eng.* 7, 943–956. <https://doi.org/10.1039/d1re00470k>.
- Zhang, Y., Zhang, S., Benson, T., 2015. A conceptual design by integrating dimethyl ether (DME) production with tri-reforming process for CO₂ emission reduction. *Fuel Process. Technol.* 131, 7–13. <https://doi.org/10.1016/j.fuproc.2014.11.006>.